# The mouse prostate: a basic anatomical and histological guideline

Daniel S. M. Oliveira[1,4], Sijana Dzinic[2,4], Alan I. Bonfil[5], Allen D. Saliganan[1], Shijie Sheng[2,3,4], R. Daniel Bonfil[1,2,3,4*]

Departments of [1]Urology, [2]Pathology, and [3]Oncology, Wayne State University School of Medicine, Detroit, MI, USA, [4]Tumor Biology and Microenvironment Program, Karmanos Cancer Institute, Detroit, MI, USA, [5]Florida International University College of Arts & Sciences, Miami, FL, USA

## ABSTRACT

Despite substantial similarities in embryological, cellular and molecular biology features, human and mouse prostates differ in organ morphology and tissue architecture. Thus, a clear understanding of the anatomy and histology of the mouse prostate is essential for the identification of urogenital phenotypes in genetically engineered mice, as well as for the study of the etiology, development, and treatment of human prostatic diseases for which mouse models are used. The purpose of this manuscript is to provide a brief guide for the dissection of the mouse prostate and the identification of its different lobes and histology, to both basic researchers and medical pathologists who are unfamiliar with mouse tissues.

KEY WORDS: Mouse models; prostate; prostate cancer; mouse prostate histology; mouse prostate anatomy

## INTRODUCTION

The prostate has a huge impact on men's health, as it is affected by diseases of significant clinical importance, such as prostate cancer, benign prostatic hyperplasia, and prostatitis [1]. Because the prostate is an accessory gland of the male reproductive system that is found only in mammals [2,3], it seems logical to use mammalian animal models to study the mechanism underlying those diseases. However, despite analogies found in prostate morphogenesis in different species [4], the variability of its anatomy among mammals is remarkable. For example, in rats and mice the prostate consists of distinct lobes, while in humans and dogs is a compact solitary structure [5,6]. Moreover, some prostate diseases commonly occurring in man are only seen in certain species, but not in others. For example, the dog is the only animal known to develop spontaneous prostate cancer that can metastasize to bone, as seen in humans [6,7]. Despite these differences, the mouse continues to be the most widely used animal model to study biological and pathological aspects of prostate, due to advantages that include its small body size, easy breeding,

short gestation time, cost-effectiveness, similarity with human genome (approximately 95% identical) and, more importantly, ease of genetic manipulation [8-12]. Indeed, the mouse has been used as a model to study prostate morphogenesis [13-19], prostatitis [20,21], and prostate cancer [22-24]. In this manuscript, we outline the anatomy and histology of the normal mouse prostate in an attempt to provide a brief but comprehensive guide to basic researchers and clinical pathologists who use this species to study prostate development and function, key molecular mechanisms leading to prostatic diseases, and/or new treatment modalities.

### Dissection of the mouse prostate

In order to obtain optimal tissue quality, the mouse prostate should be dissected *en bloc*, together with the urethra, bladder, seminal vesicles, ampullary glands, and proximal vas deferens (a.k.a. ejaculatory ducts). This is done immediately after euthanasia of the mouse using institution-approved methods. After securing the mouse on its back with the extremities pinned to the dissecting board, the fur is wet with 70% ethanol to prevent interference from loose hair during the dissection. Then, the skin is cut along the ventral midline with fine scissors. The incision should start at the area anterior to the urethral meatus using forceps to lift the skin, so that an opening can be made without damaging the underlying abdominal muscle wall. The midline incision is continued by divulsion with

blunt-pointed scissors up to the xiphoid process, followed by additional incisions to amplify the surgical fields (Figure 1A). After pinning the skin flaps to the dissecting board, an incision is made through the *linea alba* using Metzenbaum scissors to access the abdominal cavity. At this point, the urogenital tract will come into view (Figure 1B). With the help of dissecting forceps, the bladder is lifted (Figure 1C), so that the urethra, vas deferens, and ureters can be sectioned. In this way, the bladder and reproductive tract (except for the testes) are collected as a unit. The organs are then transferred to a Petri dish containing phosphate buffer solution for inspection under a dissecting microscope.

## Mouse versus human prostate anatomy

In mice, the prostate is not a single anatomical structure, but an organ comprised of four lobes located circumferentially around the urethra. These lobes, named after their spatial orientation, are the anterior, dorsal, ventral, and lateral lobes, and can be distinguished from each other using a dissecting microscope (Figure 2A-D). Anterior to the urethra and caudal to the bladder, the ventral prostate (VP) can be recognized



**FIGURE 1.** Mouse dissection and excision of the male urogenital tract. (A) Adult male mouse in supine position. Dashed lines indicate the skin incision pattern to follow; (B) Bladder (below cotton swab) and seminal vesicles (arrow) are easily identified once the abdominal cavity of the mouse is opened; (C) Most of the urogenital tract can be harvested from the mouse carcass *en bloc* by grasping the bladder with tweezers, pulling it up, and cutting the base of the urethra (arrowhead). Scale bar, 0.5 cm.

as a gelatinous pinkish structure that partially wraps the urethra ventrally, where its ducts empty. The VP is flanked by two lobes that lay on both sides of the urethra to shape the lateral prostate (LP). The butterfly-shape dorsal prostate (DP) is located bilaterally at the base of the seminal vesicles, which are easily recognized as two white horn-shape sacculated anatomic structures located dorsolateral to the bladder. LP and DP are often referred to as the dorsolateral prostate (DLP), though they present some differences in their histology (see "Histology of the Mouse Prostate" section). The anterior prostate lobes (AP), also known as "coagulating glands", are translucent and bilaterally attached to the lesser curvature of the seminal vesicles, cranially with respect to the other prostate lobes. As opposed to the human prostate, which is anchored to the bladder pelvic floor and in front of the rectum, each of the distal ends of the mouse prostate lobes floats freely in the pelvic cavity. A schematic drawing showing a lateral view of the different mouse prostate lobes and their spatial relation with other adjacent organs can be seen in Figure 2E. Additional views can be found in the "Visible Mouse Project" developed by UC Davis Center for Comparative Medicine [25].

Contrary to mice, men have a prostate without exterior lobation that contains distinct glandular regions, including a peripheral zone (PZ), a central zone (CZ), a transition zone (TZ), and a non-glandular anterior fibromuscular stroma region, each with characteristic histology [26,27]. The PZ is the area that surrounds the proximal prostatic urethra. Based on anatomic [28] and interspecies comparisons of mRNA expression signatures [29], the mouse DL prostate lobes are homologous to the human PZ, where 75-85% of prostate adenocarcinomas occur in patients [30-33]. The CZ, which is considered to be the human counterpart of the mouse AP lobes, is a cone-shaped region that surrounds the vas deferens, and occupies about 25% of the prostate volume. The TZ, a region that does not have a mouse homologue [34] and where most benign prostatic hyperplasia lesions develop in patients [33], is the smallest zone (5-10% of prostate volume) and surrounds the distal prostate urethra [35]. Thus, while in humans the urethra is completely encircled by the prostate, this is not the case in mice.

The prostate of both species originates embryologically from the urogenital sinus (UGS), an endoderm structure present in embryos during the ambisexual stage. UGS epithelial cells form solid buds that penetrate into the surrounding UGS mesenchyme in different directions around the 10th week of gestation in humans and the 17th day of gestation in mice. These precise areas outline the rudiments of the different lobes of the mouse prostate and the different zones of the human prostate described above. In humans, the prostatic buds elongate, undergo branching morphogenesis, form a lumen, and show signs of secretory differentiation by the 14th gestational
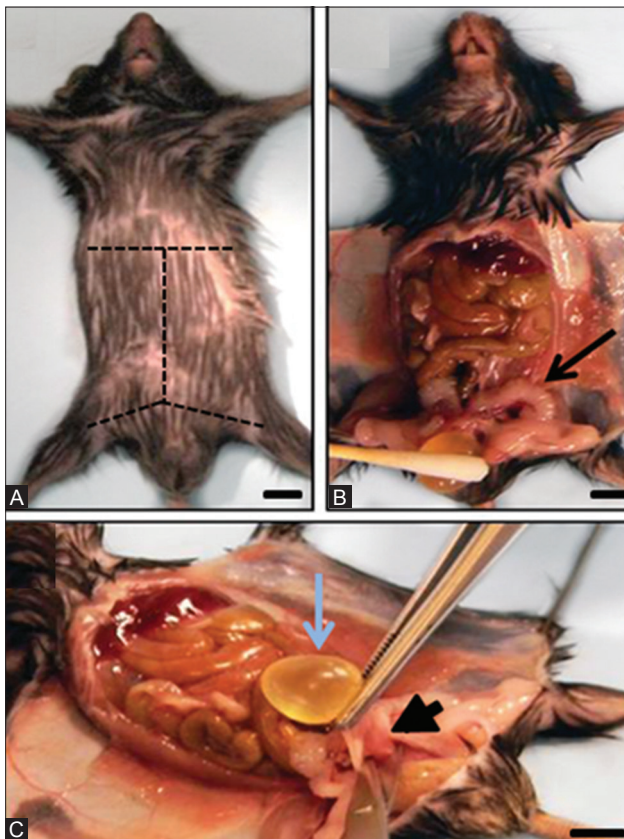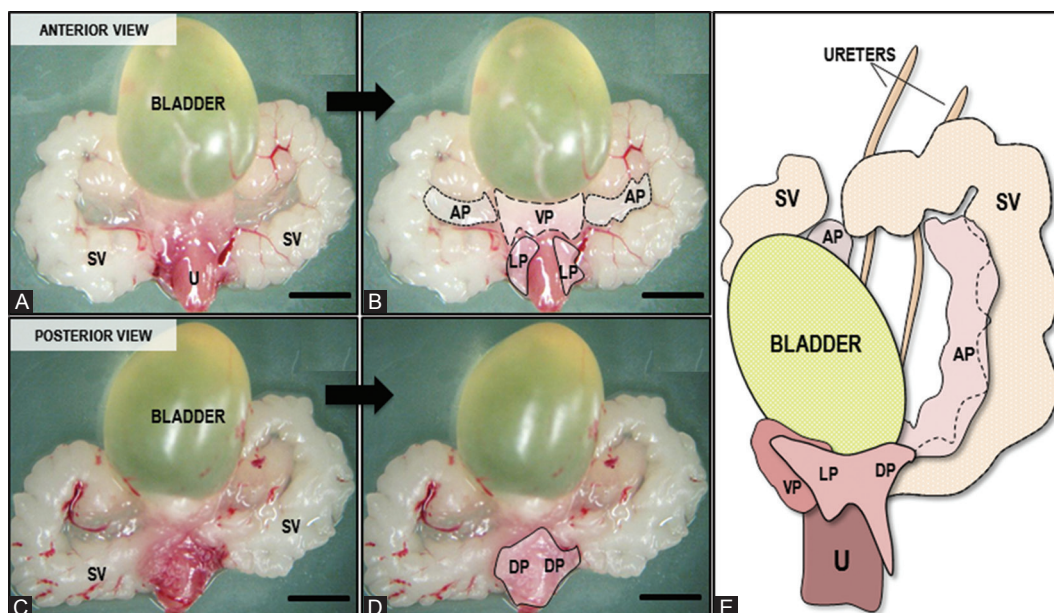
**FIGURE 2.** Gross view of mouse male urogenital organs. (A) Anterior and (C) posterior aspects of the urogenital tract dissected from an adult male mouse, as seen under the dissecting microscope. Urethra (U), Seminal vesicles (SV); (B) and (D) show the same images with dashed and dotted lines delineating the ventral (VP), lateral (LP), anterior (AP), and dorsal (DP) prostate lobes; (E) Anterolateral view (left side) of the prostate lobes relative to the bladder, seminal vesicles, and urethra (Modified from: Sugimura, Y., *et al.* [15]). Scale bar, 1 cm.

week, with an almost complete prostate development at birth. In contrast, branching morphogenesis occurs in mice postnatally, and the lobe-specific branching patterns are complete between 15 and 20 days of age [15]. In both species the prostate undergoes a rapid growth and maturation when circulating androgen levels rise at puberty (25-40 days of age in mice) (reviewed in [5]).

## Histology of the mouse prostate

Like in humans, the mouse prostate contains glands (acini) and ducts with epithelial cell types that include columnar luminal secretory cells, basal cells (less abundant and in discontinuous layers in mice), and neuroendocrine cells [34]. Luminal cells in both humans and mice are characterized by the expression of low molecular weight cytokeratin (CK) 8 and 18, and androgen receptor (AR), while basal cells express the high molecular weight CK5 and p63 in both species [3,34,36-38]. Of note, the prostate-specific antigen (PSA [kallikrein3 protein; *KLK3*, gene]) is expressed and secreted by human but not mouse luminal prostate cells, which secrete other proteins that seem to be lobe-specific [39, 40]. Neuroendocrine cells have neural and epithelial characteristics, and are found in very low numbers interspersed between basal cells present in ducts and acini, and express chromogranin A and synaptophysin [41,42]. The most conspicuous histological difference between the prostate of both species lies in the stromal component, which is very well developed in humans as an anterior fibromuscular region, whereas in mice it is sparse with minimal smooth muscle cells [34,43]. Based on publications that

include a description of the normal histology of the mouse prostate [34,42-46], here we summarize the main histological features that are essential to identify the different mouse lobes under the microscope.

All the mouse prostate lobes are surrounded by a delicate mesothelium-lined capsule, and separated from each other by fibrous and adipose connective tissue. The acini making up the prostatic lobes are surrounded by a fibromuscular tunica, and are embedded in a loose connective tissue with few stromal cells and collagen fibers [43,44]. Nerve bundles and associated ganglia are often found mainly within the connective tissue of the DLP [44]. Each of the mouse prostate lobes has distinctive histology, and can be visualized under the microscope according to their location relative to the urethra and seminal vesicles (Figure 3). The VP has moderate to large acini comprised of cuboidal to simple columnar epithelial cells, which have basally located nuclei containing small nucleoli. The luminal spaces of the VP glands are lined by a flat mucosa that presents the least amount of infolding relative to the other lobes, or some focal epithelial tufting. A thin fibromuscular layer surrounds each gland of the VP. The lumen of the glands contains homogenous pale serous secretions (Figure 4A). There is no human counterpart to the mouse VP.

The DP lobes are composed of acini small in diameter compared to the other lobes, which are lined by columnar epithelium with moderate infolding and occasional tufting, and are surrounded by a relatively dense stroma. The secretory cells have centrally located nuclei with very small or indistinct nucleoli, and their cytoplasm is lightly eosinophilic and
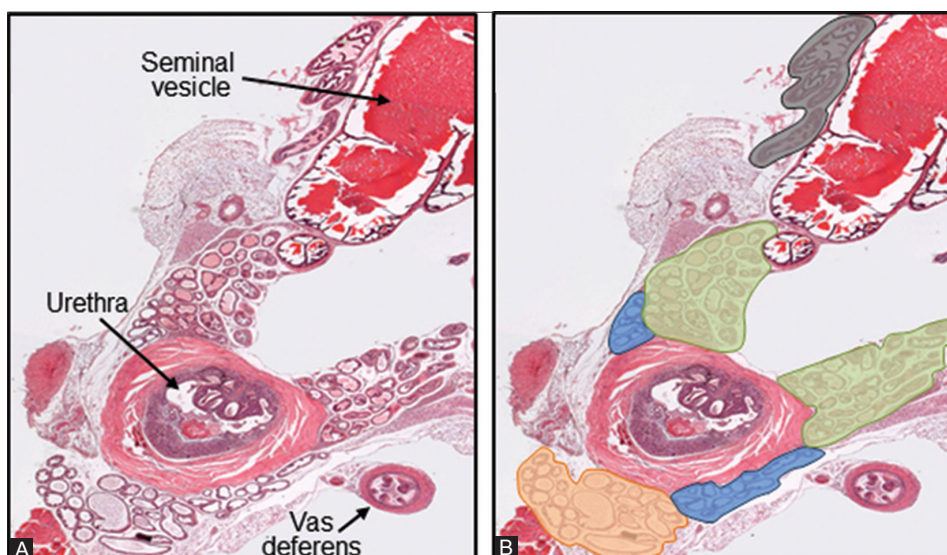
**FIGURE 3.** Cross section of a normal urogenital tract from an adult male mouse. (A) Adjacent to the prostate lobes here can be seen the urethra and a vas deferens, both surrounded by thick muscular walls, and a seminal vesicle with characteristic large lumen filled with strong esosinophilic secretion; (B) The different prostate lobes have been highlighted in orange (VP), light blue (LP), green (DP), and grey (AP), for proper identification. Hematoxylin and eosin, 25X.
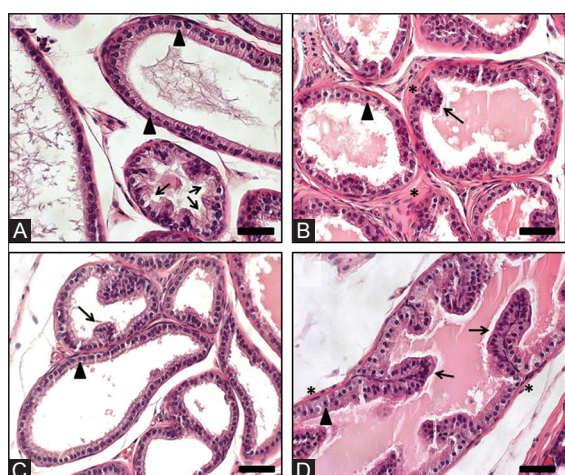


**FIGURE 4.** Mouse prostate lobes. Representative images are shown. (A) Ventral prostate: moderate to large acini are lined by cuboidal to simple columnar epithelium with flat luminal borders. Note the basally located nuclei (arrowheads) and the tufting pattern (arrows). A pale serous secretion is a unique characteristic of the ventral prostate lobe; (B) Dorsal Prostate: small acini are mostly line by simple columnar epithelium with centrally located nuclei (arrowhead) and sparse infoldings (arrow). A dense stroma (*) surrounding the acini is typical. An eosinophilic secretion is typically seen in the acini; (C) Lateral prostate: small to large acini are lined by cuboidal to low columnar epithelium with nuclei located basally (arrowhead) that form sparse infoldings (arrow). Similar to the ventral prostate, acini from the lateral prostate have a flat luminal border; (D) Anterior prostate: moderate to large acini lined mostly by cuboidal to columnar epithelium with nuclei located centrally (arrowhead) and with infoldings (arrows). Abundant eosinophilic luminal secretion is characteristic, along with the presence of noticeable smooth muscle (*) surrounding each acinus. Hematoxylin and eosin. Scale bar, 100 μm.



**FIGURE 5.** Identification of mouse prostate lobes. This decision tree suggests some key points that the basic researcher or pathologist may use to identify the different mouse prostate lobes in hematoxylin and eosin stained sections of the male mouse genitourinary tract.

granular. The luminal secretion is homogenous and eosinophilic (Figure 4B).

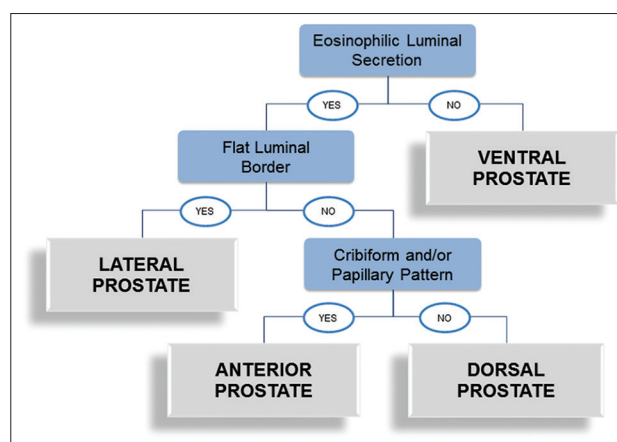The LP lobes consist of a flat luminal surface lined by cuboidal to low columnar epithelial cells that form very little infoldings. The glandular lumen may show different sizes, from small to large, and contains eosinophilic secretion. The nuclei of the secretory cells are small and located basally within an eosinophilic cytoplasm that is less granular than that of the DP (Figure 4C).

The AP or coagulating gland is characterized by complex acini that show typical papillary or cribriform patterns. The luminal space is lined by cuboidal to columnar epithelial cells, and is filled with abundant homogenous eosinophilic secretion. The nuclei of the epithelial cells are centrally located within an eosinophilic granular cytoplasm, and present a small or inconspicuous nucleolus. Each of the glands is usually surrounded by a prominent fibromuscular layer (Figure 4D).

In summary, the mouse prostate has a distinct anatomy and histology, in spite of similar embryological development,

cellular composition, and molecular characteristics to human prostate. A comprehensive understanding of the normal anatomy and histology of mouse prostate is therefore crucial to establish precise conclusions stemming from studies made with this species. In this review, we provide a simple decision tree that may aid in the identification of the different prostate lobes in histological sections of the male mouse genitourinary tract stained with hematoxylin and eosin (Figure 5).

## ACKNOWLEDGEMENTS

## REFERENCES

[1] Roehrborn C. Insights into the relationships between prostatic disorders and their potential impact on future urologic practice. Eur Urol. 2013;Suppl. 5:698-703.

[2] Luke MC, Coffey DS. The male sex accessory tissues. In: Knobil E, Nelly JD, editors. The Physiology of Reproduction. New York: Raven Press; 1994. p. 1435-89.

[3] Marker PC, Donjacour AA, Dahiya R, Cunha GR. Hormonal, cellular, and molecular control of prostatic development. Dev Biol. 2003;253(2):165-74. http://dx.doi.org/10.1016/S0012-1606(02)00031-3.

[4] Timms BG, Mohs TJ, Didio LJ. Ductal budding and branching patterns in the developing prostate. J Urol. 1994;151(5):1427-32.

[5] Prins GS, Lindgren M. Accessory sex glands in the male. In: Plant TM, Zeleznik AJ, editors. Knobil and Neill's physiology of reproduction. 1. 4th ed. London, UK: Elsevier; 2015. p. 773-804. http://dx.doi.org/10.1016/b978-0-12-397175-3.00018-1.

[6] Leroy BE, Northrup N. Prostate cancer in dogs: comparative and clinical aspects. Vet J. 2009;180(2):149-62. http://dx.doi.org/10.1016/j.tvjl.2008.07.012.

[7] Rosol TJ, Tannehill-Gregg SH, LeRoy BE, Mandl S, Contag CH. Animal models of bone metastasis. Cancer. 2003;97(3 Suppl):748-57. http://dx.doi.org/10.1002/cncr.11150.

[8] Danneman PJ, Brayton CF, Suckow MA. The Laboratory Mouse. Suckow MA, editor. United States of America: CRC Press LLC; 2000. 168 p.

[9] Rosenthal N, Brown S. The mouse ascending: perspectives for human-disease models. Nat Cell Biol. 2007;9(9):993-9. http://dx.doi.org/10.1038/ncb437.

[10] Cheon DJ, Orsulic S. Mouse models of cancer. Annu Rev Pathol. 2011;6:95-119. http://dx.doi.org/10.1146/annurev.pathol.3.121806.154244.

[11] de Jong M, Maina T. Of mice and humans: are they the same?--Implications in cancer translational research. J Nucl Med. 2010;51(4):501-4. http://dx.doi.org/10.2967/jnumed.109.065706.

[12] Maser RS, Choudhury B, Campbell PJ, Feng B, Wong KK, Protopopov A, et al. Chromosomally unstable mouse tumours have genomic alterations similar to diverse human cancers. Nature. 2007;447(7147):966-71. http://dx.doi.org/10.1038/nature05886.

[13] Cunha GR, Donjacour AA, Cooke PS, Mee S, Bigsby RM, Higgins SJ, et al. The endocrinology and developmental biology of the prostate. Endocr Rev. 1987;8(3):338-62. http://dx.doi.org/10.1210/edrv-8-3-338.

[14] Donjacour AA, Cunha GR. The effect of androgen deprivation on branching morphogenesis in the mouse prostate. Dev Biol. 1988;128(1):1-14. http://dx.doi.org/10.1016/0012-1606(88)90260-6

[15] Sugimura Y, Cunha GR, Donjacour AA. Morphogenesis of ductal networks in the mouse prostate. Biol Reprod. 1986;34(5):961-71. http://dx.doi.org/10.1095/biolreprod34.5.961

[16] Lamm ML, Podlasek CA, Barnett DH, Lee J, Clemens JQ, Hebner CM, et al. Mesenchymal factor bone morphogenetic protein 4 restricts ductal budding and branching morphogenesis in the developing prostate. Dev Biol. 2001;232(2):301-14. http://dx.doi.org/10.1006/dbio.2001.0187.

[17] Pu Y, Huang L, Birch L, Prins GS. Androgen regulation of prostate morphoregulatory gene expression: Fgf10-dependent and -independent pathways. Endocrinology. 2007;148(4):1697-706. http://dx.doi.org/10.1210/en.2006-1113.

[18] Zhou X. Roles of androgen receptor in male and female reproduction: lessons from global and cell-specific androgen receptor knockout (ARKO) mice. J Androl. 2010;31(3):235-43. http://dx.doi.org/10.2164/jandrol.109.009266.

[19] Chang C, Lee SO, Wang RS, Yeh S, Chang TM. Androgen receptor (AR) physiological roles in male and female reproductive systems: lessons learned from AR-knockout mice lacking AR in selective cells. Biol Reprod. 2013;89(1):21. http://dx.doi.org/10.1095/biolreprod.113.109132.

[20] Vykhovanets EV, Resnick MI, MacLennan GT, Gupta S. Experimental rodent models of prostatitis: limitations and potential. Prostate Cancer Prostatic Dis. 2007;10(1):15-29. http://dx.doi.org/10.1038/sj.pcan.4500930.

[21] Schwartz ES, Xie A, La JH, Gebhart GF. Nociceptive and inflammatory mediator upregulation in a mouse model of chronic prostatitis. Pain. 2015;156(8):1537-44. http://dx.doi.org/10.1097/j.pain.0000000000000201.

[22] Irshad S, Abate-Shen C. Modeling prostate cancer in mice: something old, something new, something premalignant, something metastatic. Cancer Metastasis Rev. 2013;32(1-2):109-22. http://dx.doi.org/10.1007/s10555-012-9409-1.

[23] Grabowska MM, DeGraff DJ, Yu X, Jin RJ, Chen Z, Borowsky AD, et al. Mouse models of prostate cancer: picking the best model for the question. Cancer Metastasis Rev. 2014;33(2-3):377-97. http://dx.doi.org/10.1007/s10555-013-9487-8.

[24] Wu X, Gong S, Roy-Burman P, Lee P, Culig Z. Current mouse and cell models in prostate cancer research. Endocr Relat Cancer. 2013;20(4):R155-70. http://dx.doi.org/10.1530/ERC-12-0285.

[25] Kuroda N, Naroda T, Tamura M, Perez-Montiel D, Michal M, Hes O. High-grade urothelial carcinoma, plasmacytoid variant, of the renal pelvis with osteoclast-like giant cells and focal rhabdoid features. Polish journal of pathology : official journal of the Polish Society of Pathologists. 2014;65(3):237-40. http://dx.doi.org/10.5114/pjp.2014.45788.

[26] McNeal JE. Regional morphology and pathology of the prostate. Am J Clin Pathol. 1968;49(3):347-57.

[27] McNeal JE. Prostate. In: Sternberg SS, editor. Histology for pathologists. 2nd ed. Philadelphia: Lipincott; 1997. p. 997-1017.

[28] Price D. Comparative Aspects of Development and Structure in the Prostate. Natl Cancer Inst Monogr. 1963;12:1-27.

[29] Berquin IM, Min Y, Wu R, Wu H, Chen YQ. Expression signature of the mouse prostate. J Biol Chem. 2005;280(43):36442-51. http://dx.doi.org/10.1074/jbc.M504945200.

[30] McNeal JE, Redwine EA, Freiha FS, Stamey TA. Zonal distribution of prostatic adenocarcinoma. Correlation with histologic pattern and direction of spread. Am J Surg Pathol. 1988;12(12):897-906. http://dx.doi.org/10.1097/00000478-198812000-00001.

[31] Reissigl A, Pointner J, Strasser H, Ennemoser O, Klocker H, Bartsch G. Frequency and clinical significance of transition zone cancer in prostate cancer screening. Prostate. 1997;30(2):130-5. http://dx.doi.org/10.1002/(SICI)1097-0045(19970201)30:2<130:: AID-PROS8>3.0.CO;2-S

[32] Noguchi M, Stamey TA, Neal JE, Yemoto CE. An analysis of 148 consecutive transition zone cancers: clinical and histological characteristics. J Urol. 2000;163(6):1751-5. http://dx.doi.org/10.1016/S0022-5347(05)67535-0

[33] De Marzo AM, Platz EA, Sutcliffe S, Xu J, Gronberg H, Drake CG, et al. Inflammation in prostate carcinogenesis. Nat Rev Cancer. 2007;7(4):256-69. http://dx.doi.org/10.1038/nrc2090.

[34] Roy-Burman P, Wu H, Powell WC, Hagenkord J, Cohen MB. Genetically defined mouse models that mimic natural aspects of

human prostate cancer development. Endocrine-Related Cancer. 2004;11(2):225-54. http://dx.doi.org/10.1677/erc.0.0110225.

[35] Bostwick DG, Cheng L. Urological Surgical Pathology. 3rd ed. Philadelphia: Elsevier Health Sciences; 2014.

[36] Zhang C, Guo Y, Cui J, Zhu HH, Gao WQ. Cytokeratin 18 is not required for morphogenesis of developing prostates but contributes to adult prostate regeneration. Biomed Res Int. 2013;2013:576472. http://dx.doi.org/10.1155/2013/576472.

[37] Lee SO, Tian J, Huang CK, Ma Z, Lai KP, Hsiao H, et al. Suppressor role of androgen receptor in proliferation of prostate basal epithelial and progenitor cells. J Endocrinol. 2012;213(2):173-82. http://dx.doi.org/10.1530/JOE-11-0474.

[38] Lawson DA, Xin L, Lukacs RU, Cheng D, Witte ON. Isolation and functional characterization of murine prostate stem cells. Proc Natl Acad Sci U S A. 2007;104(1):181-6. http://dx.doi.org/10.1073/pnas.0609684104.

[39] Diamandis EP, Yousef GM, Olsson AY. An update on human and mouse glandular kallikreins. Clin Biochem. 2004;37(4):258-60. http://dx.doi.org/10.1016/j.clinbiochem.2003.12.013.

[40] Fujimoto N, Akimoto Y, Suzuki T, Kitamura S, Ohta S. Identification of prostatic-secreted proteins in mice by mass spectrometric analysis and evaluation of lobe-specific and androgen-dependent mRNA expression. J Endocrinol. 2006;190(3):793-803. http://dx.doi.org/10.1677/joe.1.06733.

[41] Zhou Z, Flesken-Nikitin A, Nikitin AY. Prostate cancer associated with p53 and Rb deficiency arises from the stem/progenitor cell-enriched proximal region of prostatic ducts. Cancer Res. 2007;67(12):5683-90. http://dx.doi.org/10.1158/0008-5472.CAN-07-0768.

[42] Knoblaugh S, True L. Male reproductive system. In: Treuting PM, Dintzis SM, editors. Comparative anatomy and histology A mouse and human atlas. 1st ed. London, UK: Academic Press; 2012. p. 285-308. http://dx.doi.org/10.1016/B978-0-12-381361-9.00018-4.

[43] Shappell SB, Thomas GV, Roberts RL, Herbert R, Ittmann MM, Rubin MA, et al. Prostate pathology of genetically engineered mice: definitions and classification. The consensus report from the Bar Harbor meeting of the Mouse Models of Human Cancer Consortium Prostate Pathology Committee. Cancer Res. 2004;64(6):2270-305. http://dx.doi.org/10.1158/0008-5472.CAN-03-0946.

[44] Harmelin A, Danon T, Kela I, Brenner O. Biopsy of the mouse prostate. Lab Anim. 2005;39(2):215-20. http://dx.doi.org/10.1258/0023677053739756.

[45] Scudamore CL. Reproductive system. In: Scudamore CL, editor. A practical guide to the histology of the mouse. Hoboken, NJ: Wiley Blackwell; 2014. p. 87-107. http://dx.doi.org/10.1002/9781118789568

[46] Suwa T, Nyska A, Haseman JK, Mahler JF, Maronpot RR. Spontaneous lesions in control B6C3F1 mice and recommended sectioning of male accessory sex organs. Toxicol Pathol. 2002;30(2):228-34. http://dx.doi.org/10.1080/01926230275 3559560.